24th COBEM - 2017

24th ABCM International Congress of Mechanical Engineering
December 3-8, 2017, Curitiba, PR, Brazil

COBEM-2017-5912
NUMERICAL SIMULATION OF AIR-SOLID THERMAL STORAGE FOR CSP SYSTEMS

Claudio Adasme
Taygoara Oliveira
Antonio Brasil Junior
Mario Siqueira
Universidade de Brasilia, Department of Mechanical Engineering, Brasilia, Brazil
claudioadasme@vtr.net, taygoara@unb.br, brasiljr@unb.br, mariosiqueira@unb.br

Abstract. *This work presents the results of a numerical modeling of a porous ceramic honeycomb for sensible thermal energy storage. An air-solid two equation lumped model for a porous medium, which considers convection and conduction heat transfer, is formulated and solved numerically. In order to obtain the convective heat transfer coefficient, several 3D simulations in Star-ccm+ are performed, and an empirical Nusselt Reynolds correlation is proposed for a single honeycomb channel. The correlation is evaluated in the model locally considering variable thermo-physical properties for the heat transfer fluid in order to obtain the convective coefficient. Then, the resultant coefficient is extrapolated for the entire honeycomb matrix and validated through a CFD simulation of a thermal loading cycle. The numerical model results show a good agreement with the CFD simulation for the fluid temperature and the amount of the energy stored by the solid.*

Keywords: *ceramic honeycomb, thermal storage, porous media, sensible heat, CSP*

1. INTRODUCTION

Concentrating solar power system (CSP) technology has proven to be an important alternative as renewable power generation. The integration of a thermal energy storage (TES) system allows it to improve its performance and reliability by reducing the mismatch between energy supply and energy demand. TES system are classified as latent heat, sensible heat or thermo-chemical heat storage (Kuravi *et al.*, 2013), part of the advantages of sensible heat storage in materials like ceramic solid matrix are its simplicity, low cost and its ability of storage energy at high temperatures (Dominik Schilpf, 2014).

The numerical model proposed in this work is based in the heat governing equations for a porous media and considers a local thermal non-equilibrium between the fluid and de solid phase (Nield and Bejan, 2006). Initially proposed by Schumann in 1929, it has been widely used for modeling thermal storage in packed beds (Agalit *et al.*, 2015; Andreozzi *et al.*, 2014; Zanganeh *et al.*, 2015; Cascetta *et al.*, 2015; Hänchen *et al.*, 2011).

There are many publications witch studied this model, Coutier and Farber (1982) applied them to a packed bed as storage unit for an air based solar system, on their work was described the heat transfer process between the fluid and solid phase. The volumetric convective heat transfer coefficient was obtained by comparing the model results and experimental tests. More recent publications are related with the application of this model for heat storage systems integrated to a CSP power plant, they focused on describing the dynamic behavior considering the operational conditions of CSP technology. Thus higher fluid temperatures and pressures were considered, efficiency criteria were defined, different materials were studied and continuous thermal charge and discharge cycles were performed. Moreover other parameters have been incorporated as the heat loss through the walls in the form of natural convection or the heat transfer by thermal radiation for higher temperatures.

In that way, Hänchen *et al.* (2011) considered a inlet fluid at 800K and their investigated on the overall thermal efficiency as function of the mass flux, storage material and total length of the TES. Then Zanganeh *et al.* (2015) explored a different geometry for the TES and validated the model using experimental data for a 6,5 MWhth pilot scale TES. Agalit *et al.* (2015) increased the operating temperature and pressure up to 1000K and 10 bar respectively. Due this increment they considered variables thermo-physical properties for both fluid and solid phases. All those researches were focused on packed beds configuration as TES and for the volumetric convective heat transfer coefficient they used the experimental expression proposed by Coutier and Farber (1982).

Another approach to define the volumetric convective coefficient was used by Cascetta *et al.* (2015, 2016). They

used an empirical Nusselt-Reynolds-Prantdl correlation especially proposed for packed beds, the experimental test was performed at a relative low temperature (573 K). The numerical model was compared with a 2D axis-symmetrical CFD simulation and the experimental test, showing a good agreement. They conclude that the main advantage of the numerical model is the low computational cost and a good predicting axial temperature but in counterparts the model was not accurate for energy storage prediction. All works mentioned used empirical correlation for the convective heat transfer coefficient, especially proposed for packed beds configurations with good results when compared with experimental data.

For porous structures like honeycomb, Andreozzi *et al.* (2014) implemented the two equations model in a 2-D axis-symmetrical CFD simulation, the heat transfer coefficient was initially obtained by 3D simulation for one channel only, then this coefficient was extrapolated to the entire solid matrix. Their work focused in the thermal radiation effect in the change and discharge cycles and the effect of porosity.

This work investigate the implementation of this model to a honeycomb porous structure. Unlike the study performed by Andreozzi *et al.* (2014), this work resolves the 1D equations numerically by using differences finites method in Matlab R2015. Another particularity of this work is each channel has a variable cross section, due this geometry this work proposes an approach to obtain the volumetric convective heat transfer coefficient trough CFD simulations on a reduced domain.

2. METHODOLOGY

2.1 Physical Domain

The physical domain under investigation consists in a cubic solid matrix with parallel channels as shown in figure 1a. The air passing through the channels initiates a process of heat exchange with the solid and, as long as the fluid temperature is higher than the matrix, the solid raises its temperature, thus the matrix operates as sensitive heat storage system. The model considers this domain as a porous media wherein the parallel channels will conform the void fraction. The main purpose of the porous structure is to obtain convective heat transfer enhancement between the fluid and the solid storage material. Several studies has been published reporting convective transfer improvement in variable diameter ducts Russ and Beer (1997); Nishimura *et al.* (2003); Mahmud *et al.* (2003). Hence each channel has a periodically varying cross section as shown in figure 1b.

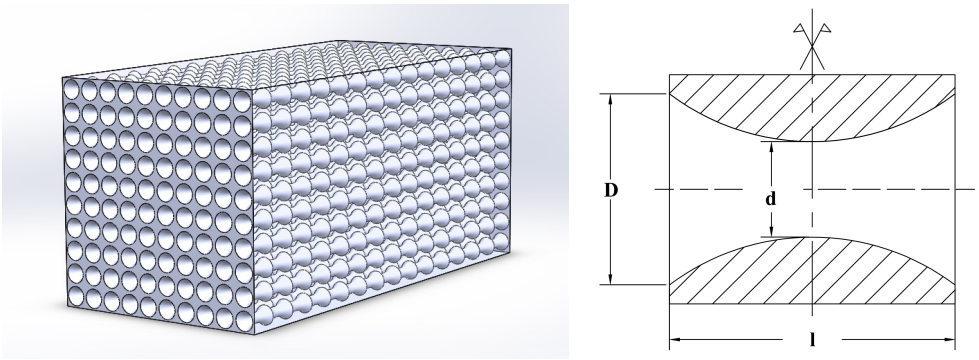

(a) Physical domain proposed

(b) periodic channel section

Figure 1: Porous matrix geometry

2.2 Simplified numerical model

In order to investigate the thermal behavior of the porous media, the proposed model will consist of two-phase lumped transient energy equations, described by the energy balance equation for a porous medium. These equations consider a local thermal non-equilibrium (LTNE) and are given as follows:

For the fluid phase (f):

$$\varepsilon \cdot \left(\rho_f C_{p,f}\right)\frac{\partial T_f}{\partial t} + C_{p,f} G \frac{\partial T_f}{\partial x} = h_v\left(T_s - T_f\right) \tag{1}$$

For the solid phase (s):

$$\left(1-\varepsilon\right)\cdot\left(\rho_s C_{p,s}\right)\frac{\partial T_s}{\partial t} = h_v\left(T_f - T_s\right) + \left(1-\varepsilon\right)k_s\frac{\partial^2 T_s}{\partial x^2} \tag{2}$$

where:

ε = void fraction of the porous media;

ρ = density of fluid (f) or solid (s) (kg/m^3);
C_p = Specific heat of fluid (f) or solid (s) (J/kgK);
T = temperature of fluid (f) or solid (s) (K);
t = time (s);
x = axial direction (m);
G = mass flow rate for unit cross section (kg/m^2s);
k = thermal conductivity of fluid (f) or solid (s) (W/mK);
h_v = Volumetric convective heat transfer coefficient (W/m^3K).

The equations above represent a simplified one-dimensional model, which aims to obtain both solid and fluid temperatures along the longitudinal axis, considering a uniform radial temperature distribution. The model focused on the convective heat transfer between the phases and considers heat conduction through the solid phase in the flow direction. Theses equation are linked by the volumetric heat convection coefficient so the fluid temperature changes in time and space due to convective heat exchange with the solid phase, as the process of heat transfer takes place only between the solid and the air, the internal energy change take effect simultaneously on both phases.

The model described above is based on the following assumptions:

- The heat transfer fluid (HTF) is air, and its thermo-physical properties such as density, viscosity, specific heat and thermal conductivity are variable.
- Solid thermo-physical properties are considered as constants.
- Temperature gradient in the radial direction is disregarded.
- There is no internal heat generation and no mass transfer.
- Radiative heat transfer is assumed negligible.
- Heat loss from the outer walls of the solid to the environment is disregarded.
- Heat conduction in the fluid phase is neglected.

The equations will be solved using the finite elements method and the variables time t and the axial direction x will be discretized for each time and spatial step fluid and solid temperature values will be computed. The initial and boundary conditions are the following:

- The initial fluid and solid temperature distribution must be specified.
- The inlet fluid temperature T_f, and the mass flow G will be constant in time.
- Adiabatic condition for the fluid at the exit of the domain.
- Adiabatic condition for the solid at the entrance and exit of the domain.Thus, there will be no heat transfer trough the cross surface at the inlet and outlet of the porous media

Regarding the thermo-physical properties of air, the relations proposed by Agalit *et al.* (2015) will be applied in this work, considering a constant operating pressure of 1 bar. These properties will be calculated at every time step and position.

2.3 Convective heat transfer coefficient

The volumetric convective heat transfer coefficient h_v will be evaluated indirectly through CFD simulations of a single channel. The volumetric coefficient is related to the single channel coefficient h_{ch} by the interface area per volume a_{sf} defined as (Andreozzi *et al.*, 2014):

$$a_{sf} = \frac{\text{Interface area}[m^2]}{\text{Porous media volume}[m^3]} \tag{3}$$

So the volumetric volumetric convective heat transfer coefficient h_v can be defined as:

$$h_v = a_{sf} h_{ch} \tag{4}$$

With this approach, the convective channel coefficient h_{ch} can be obtained assuming the principles of internal forced convection of a turbulent flow in a duct.This domain reduction also reduces the use of computational resources to carry out the simulations.

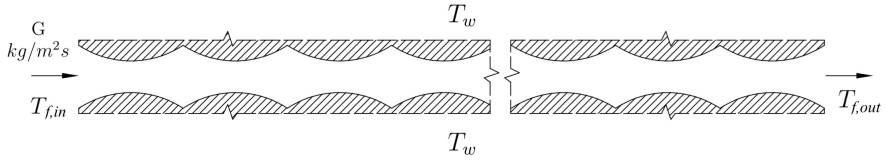

Figure 2: Single matrix porous channel

The figure 2 shows the single channel domain, in order to evaluate the mean outlet fluid temperature $T_{f,out}$, constant wall temperature T_w is imposed at the fluid-solid interface surface. Additionally, for the fluid is defined a constant mean inlet temperature $T_{f,in}$ and a constant flow rate $\dot{m}$. Thus, by conservation of energy, the heat rate q exchanged by the fluid can be defined as:

$$q = \dot{m} C_{p,f} (T_{f,out} - T_{f,in}) \tag{5}$$

As the surface temperature T_w is considered as constant, the Newton's law of cooling, the heat rate can be expressed as (Incropera, 2013):

$$q = h_{ch} A \Delta T_{lm} \tag{6}$$

Where A is the interface area of heat exchange and T_{lm} is the logarithmic mean difference for a turbulent duct flow (Incropera, 2013). By equating (5) and (6), the experimental value of the heat transfer channel coefficient can be expressed as:

$$h_{ch} = \frac{\dot{m} C_{p,f} (T_{f,out} - T_{f,in})}{A \Delta T_{lm}} \tag{7}$$

In parallel, as known, the Nusselt number could be defined as:

$$Nu = \frac{h_{ch} d_m}{k_f} \tag{8}$$

where k_f is the fluid thermal conductivity and d_m is the mean diameter for the channel. As the internal diameter is variable, it will be considered a mean constant diameter given by the following expression:

$$d_m = \frac{A}{\pi L} \tag{9}$$

where L is the channel total length.

Additionally, it possible to relate the Nusselt number to Reynolds and Prantdl numbers by using an empirical correlation expressed as $Nu = aRe^m Pr^n$. Hence, as a procedure discussed by Holman (2010), using different flow rates it is possible to obtain a series of data that can lead us to the values of coefficients a, m and n.

Then, once obtained the correlation coefficients, it will be possible to formulate the heat transfer coefficient of the channel as a function of Reynold and Prantdl numbers:

$$h_{ch} = \frac{aRe^m Pr^n}{k_f} \tag{10}$$

Finally, with the coefficient h_{ch} it is possible to obtain the fluid temperature along the channel by solving the following differential equation Incropera (2013).

$$\frac{dT_f}{dx} = \frac{h_{ch} \pi d_m}{\dot{m} C_{p,f}} (T_w - T_f) \tag{11}$$

2.4 CFD simulations

The simulations in CFD were performed in commercial software Star-ccm+ version 10.06.010. Several steady state simulations will be performed in order to obtain the empirical Nusselt-Reynolds correlation with the coefficients a, m, n. The figure 3 illustrates the complete domain defined for the simulations and its boundary conditions and figure 4 illustrates

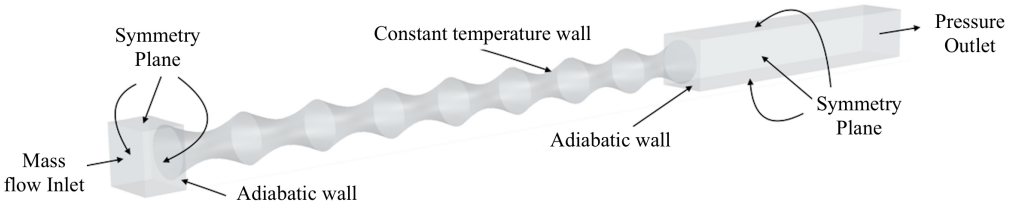

Figure 3: Physical domain for CFD simulations and boundary conditions

its dimensions. The domain at the inlet and outlet has a square H-side cross section, the dimension H corresponds to the distance between one channel to the other, so this section is identical to any other in the matrix.

The L_{in} and L_{out} correspond to the inlet and outlet diffusers lengths, defined with the aim that the boundary conditions do not interfere in the development of the flow. Since the stationary simulations consist in an internal flow with constant wall temperature T_w, the domain does not consider the volume of the solid around the channel, but only the interface surface with the fluid. The simulated case represents an inner channel and the same assumptions considered to the mathematical model applied.

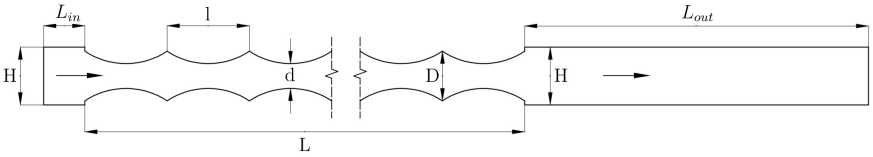

Figure 4: Single channel main dimensions

The simulations were performed for a series of different lengths L and flows G; the remaining parameters such as L_{in}, L_{out} and channel geometry were kept constant. Table 1 shows a summary of the parameters used in the simulations. For

Table 1: Operational parameters

Parameter	value	Parameter	value
D	0,06 m	L_{out}	0,7 m
d	0,03 m	T_{in}	800 K
l	0,1 m	T_w	300 K
H	0,07 m	L	$[1,0; 6,0]$ m
L_{in}	0,05 m	G	$[0,2; 0,55] kg/m^2 s$

lengths above 3.0 m, the domain shown in figure 3 was reduced, by dividing the channel in half with a symmetry plane. This domain reduction compensates the increase of the numerical mesh due to the longer length, thus limiting the amount of mesh cells, and avoiding and excessive extension of computational processing time.

2.5 CFD Transient state-Conduction convection coupled simulation

Unsteady simulation consists on temperature evolution of both fluid and solid phase over time performed to validate the model. In this case, the interface surface temperature is no longer constant but evolves according to the difference with temperature fluid, the convection coefficient and the thermo-physical properties of the solid. In this way, the simulation domain incorporates the volume of the solid around the channel contained in the square section HxH. The solid material is made of steatite and its properties are summarized in table 2.

Table 2: Thermophysical properties of Steatite

Density $\rho_s(kg/m^3)$	Specific heat $C_s(J/(kgK))$	Conductivity $k_s(W/(mK))$
1068	987	2,5

Since the volume of the solid is being added in this domain, the number of cells in the volumetric mesh is greater than in the steady state simulations. The initial domain of figure 3 was divided by two longitudinal symmetry planes perpendicular to each other, reducing the domain to one quarter of the complete channel as shown in figure 5.

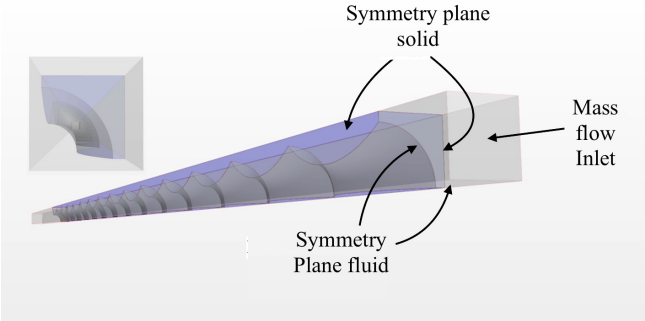

Figure 5: Single channel domain for unsteady simulation

As the convective heat transfer occurs at the interface surface between the fluid and the solid, it is important that the effects of the boundary layer and laminar sublayer be correctly captured in order to obtain the correct value for the phenomenon to be simulated. In this way, the value of the convective coefficient depends strongly on how the turbulence model solves the flow in the region near the wall. In this work, the k-omega SST turbulence model is used with mean values of y^+ close to 1 and maximum below to 5 as recommended in literature Andersson (2012). For mesh sensitivity analysis, several configurations were tested until to obtain a convergence in fluid temperature at the outlet.

3. RESULTS AND DISCUSSION

For the steady state simulations performed, the mean outlet temperature was obtained for each case. With this value is possible to determine the Nusselt number according equations (7) and (8). Additionally, for each simulation, the Prantdl Pr number computed was approximately a constant value ($Pr = 0703$). Thus, the Prantdl number exponent n was considered as $1/3$ and, the resulting correlation to obtain the coefficients a and m for a channel length $L = 1,5m$ is shown in the figure 6.

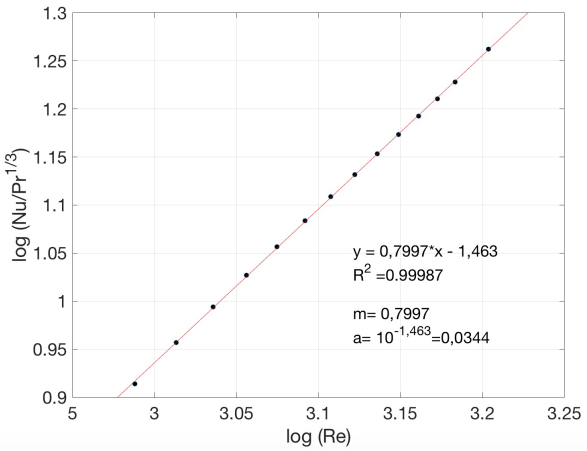

Figure 6: log-log plot for Reynolds-Nusselt correlation $L = 1,5m$

Finally, equation (10) can be written, for the case of $L = 1,5m$ as:

$$h_{ch} = \frac{0,0344 Re^{0,7997} Pr^{\frac{1}{3}}}{k_f} \tag{12}$$

If the total channel length is large compared to the entrance length, then the effect of the entrance length can be neglected. In order to define the minimum length where this effects are not relevant, several simulations were performed for a range of channel lengths. Therefore, the resultant coefficients for each of them are shown in figure 7.

In figure 7a, it can be noticed that as the length of the channel increases, there is a stabilization of the value of coefficient a. On the other hand, in figure 7b the coefficient m remains invariable for all lengths simulated. So can be concluded that the effect of the development entry region in not relevant since $L = 3$ meters. Generalizing, for this geometry it is possible to propose the Nusselt-Reynolds relation for fully developed turbulent flows according to the following equation:

$$Nu = 0,036 Re^{0,8} Pr^{1/3} \tag{13}$$

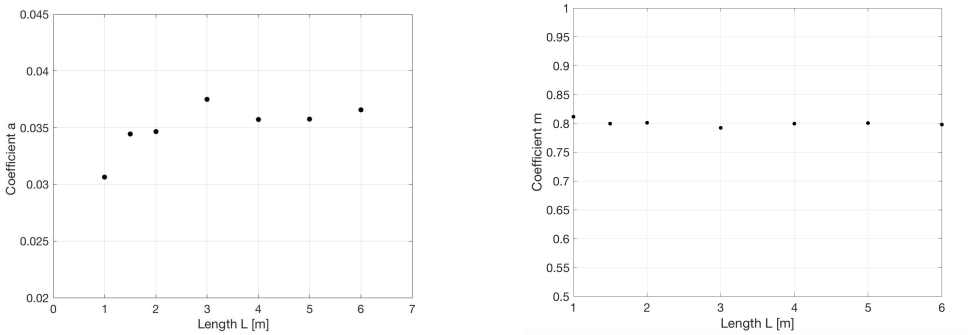

(a) Coefficient a (b) Coefficient m

Figure 7: Coefficients a e m obtained from steady state simulations

A traditional expression for the Nusselt number is the Colburn equation Çengel (2003), witch refers to the Nusselt-Reynolds correlation for a fully development turbulent flow in a smooth circular tubes (equation (14)).

$$Nu = 0,023 Re^{0,8} Pr^{1/3} \tag{14}$$

If we compare the coefficients obtained with those proposed by Colburn, its noticeable that the Reynolds number exponent are similar to those proposed by Colburn. The difference lies on the multiplier factor a, which is greater than proposed by Colburn for the smooth tube, this value confirms the heat transfer enhancement wanted. This results are consistent with the findings of Rush *et al.* (1999); Wang and Chen (2002); Mahmud *et al.* (2003); Nishimura *et al.* (2003) related with sinusoidal section tubes researches.

The fluid temperature for the steady simulations were compared with results obtained using the equation (11) solved with the Euler method and the computed correlations for h_{ch}.

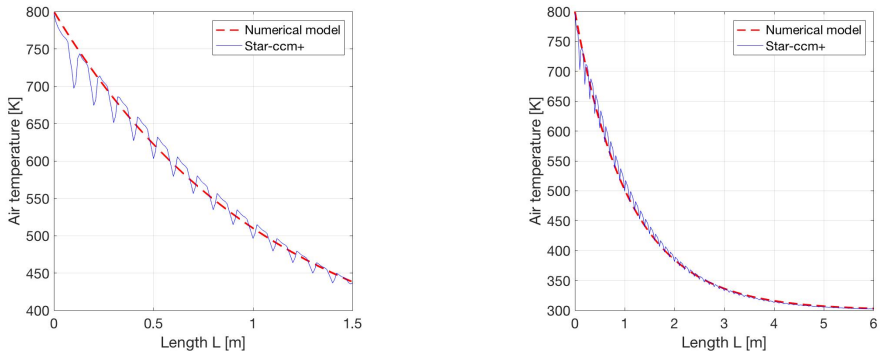

(a) L=1,5 m for G= 0,5 kg/m^2s (b) L=6,0 m for G= 0,5 kg/m^2s

Figure 8: Fluid temperature profile along longitudinal axis

From the figures above, it can be observed that there is a good agreement between the numerical results and the simulations performed in Star-ccm+. There is a disagreement between the curves at the entrance of the channel which is more noticeable with length $L = 1,5m$, this difference can be explained because the entrance region effects are disregarded by the numerical results but they are correctly resolved by the simulations. Nevertheless, all curves accurately predict the outlet fluid temperature, which is one of the most important parameter for the thermal energy storage modeling.

3.1 Friction factor

The friction factor of Darcy f is defined by the Darcy-Weisbach equation, which as a function of pressure loss, and can be written as:

$$f = \frac{2 \cdot \Delta P \cdot d}{L \cdot \rho_f \cdot u^2} \tag{15}$$

The figure 15 represents the relation between the friction factors computed with the simulations data and the corresponding Reynolds number. It seems that the friction factors, represented in the Moody chart, forms a straight line with a similar slope than the curve for a straight tube with 0,07 of relative roughness. It is possible to see a clear pattern of points forming

a line that responds to the power law indicated in the same graph. The resulting equation is similar to that proposed by Mahmud *et al.* (2003), and as they reported the friction factor also resulted larger than the corresponding one for a straight wall tube. Wang and Chen (2002) adjudicates this increment in pressure drop to the shear stress of the wall in sections where the diameter decreases to the minimum value.

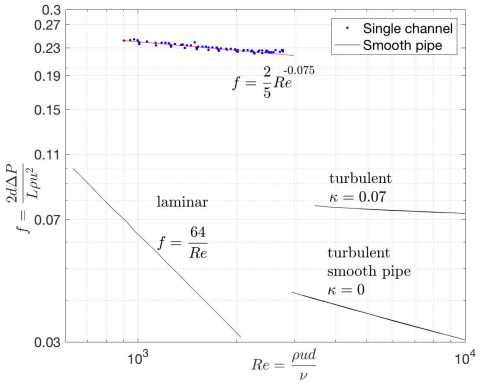

Figure 9: Friction factor as a function of Reynolds number

3.2 Model validation

The unsteady simulation was performed for one thermal load cycle, the initial temperature of both phases was defined as 300 K, with a constant air flow of $G = 0,225\ kg/m^2s$ in a porous matrix with length $L = 1,5m$. The others operating parameters remained constant according to table 3.2.

Figure 10 shows a comparison between the numerical model and the CFD simulation for a charging cycle of 4500 seconds. In the figure, are shown the temperatures profiles along the axis for both phases at the end of the charging cycle. The difference between the fluid temperature curves is similar than the constant wall temperature case, wherein is also possible to observe the difference at entry region with a good convergence at outlet.

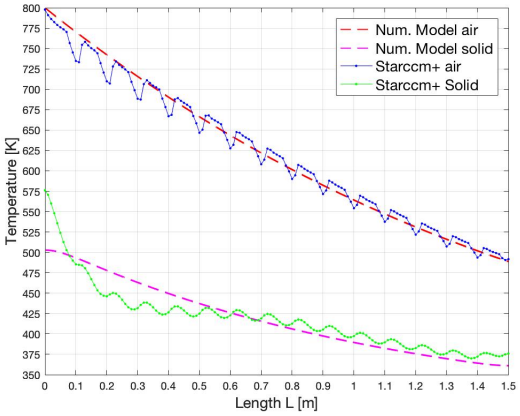

Figure 10: Final porous media temperature after 4500 s of charging.

For solid temperatures, the differences are larger, the curve obtained from Star-ccm + presents a sinusoidal trajectory, as expected due to the channel geometry, in this curve the high temperature points correspond to the region downstream of the larger diameters, precisely where the flow starts to be directed to the smaller section diameter, and a fraction forms the a recirculation vortex as shown in figure 11. On the contrary, the numerical model assumes a constant diameter so the curve looks similar to any pipe internal flow.

The figure 12a shows the evolution in time of the fluid temperature, there is good agreement in time between the models and the simulation results. As illustrates the figure 12b, the difference seems to remain constant and 1% along the entire charging cycle.

The energy stored by the solid is defined by the difference between its energy at the beginning of the cycle $(t = 0)$ and its energy at the end of the cycle. So the stored energy at the end of the charging cycle will be given by the following equation:

$$E = \rho_s C_s \int_0^L A(x)(T_{s,x}^{final} - T_{s,0})dx \tag{16}$$

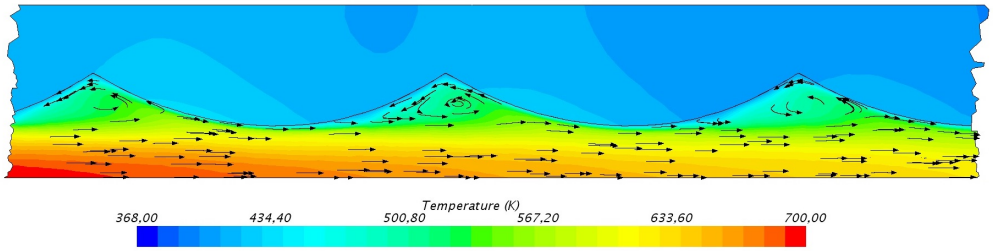

Figure 11: Streamlines and Fluid and solid temperatures for a middle section of channel

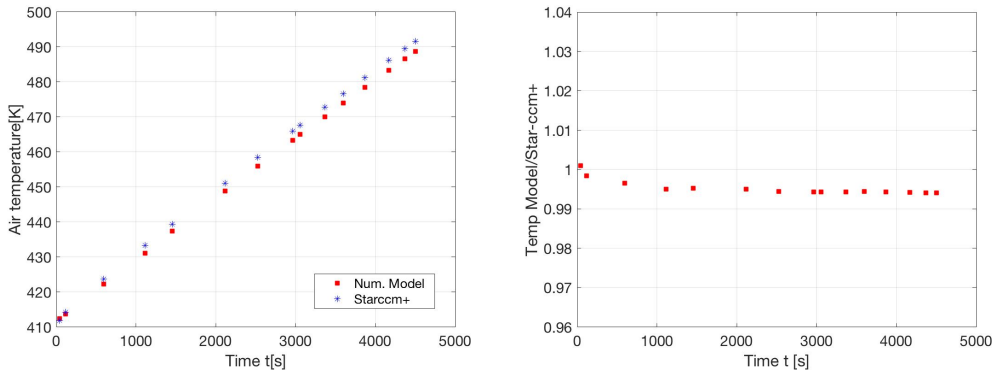

(a) Outlet temperature difference (b) Outlet temperature desviation

Figure 12: Time evolution of outlet temperature during thermal load cycle

Figure 13 represents a comparison in time of the energy stored by the solid between Star-ccm+ and the numerical model, in which the energy calculated by the mathematical model differs from the simulation in less than 1%. The energy stored by the fluid is neglected in both, numerical model and CFD simulation.

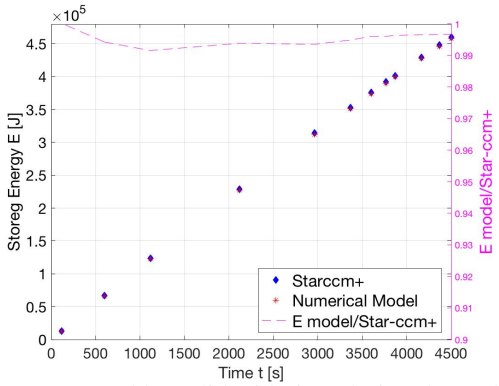

Figure 13: Energy stored by solid with time during thermal load cycle

In this way, we have that the mathematical model is a good predictive tool for fluid temperature. The good agreement between the stored energy compensates the difference in the solid temperature profile. This difference, should be studied more in detail with the aim of verify that in thermal discharge process, where the flow is inverted, the fluid temperature values do not differ more than tolerable.

4. CONCLUSIONS

A two equation lumped simplified model was proposed for a porous honeycomb matrix. The model was numerically investigated taking special attention in the volumetric heat coefficient.

The results in term of temperature profile are in good agreement with the CFD simulation, especially for the fluid phase. For solid phase the storage energy values also shown a good accuracy. Difference of temperature at entrance region could be explained because the Reynols analogy is proposed to be used in fully development flow sections so, by extending the honeycomb length it could be possible to minimize that difference.

The approach proposed to evaluate the volumetric heat transfer coefficient is highly reproducible for other honeycombs

configurations and the correlation obtained are coherent with other correlations proposed in the literature.The extrapolation of the channel convection coefficient seems to be adequate cause both the steady state and the transient model seems to show same leves of accuracy.

In that way, the model proposed, in conjunction with the methodology for calculating the heat transfer coefficient, could be an important tool to evaluate different honeycomb configurations, performing severals operating thermal cycles of charge and discharge with a low computational cost and time consumption compared with CFD tools. Then, overall performance can be investigated and another parameters as thermal radiation or heat loss can be added to the model in order to have more realistic results.

5. ACKNOWLEDGEMENTS

This work was supported by CNPq research project 407076/2013-1.

6. REFERENCES

Agalit, H., Zari, N., Maalmi, M. and Maaroufi, M., 2015. "Numerical investigations of high temperature packed bed tes systems used in hybrid solar tower power plants". *Solar Energy*, Vol. 122, p. 603âĂŞ616. doi: 10.1016/j.solener.2015.09.032.

Andersson, B., 2012. *Computational fluid dynamics for engineers*. Cambridge University Press.

Andreozzi, A., Buonomo, B., Manca, O. and Tamburrino, S., 2014. "Thermal energy storages analysis for high temperature in air solar systems". *Volume 71: Applied Thermal Engineering*. doi:10.1115/imece2012-88891.

Cascetta, M., Cau, G., Puddu, P. and Serra, F., 2015. "A study of a packed-bed thermal energy storage device: Test rig, experimental and numerical results". *Energy Procedia*, Vol. 81, p. 987âĂŞ994. doi:10.1016/j.egypro.2015.12.157.

Cascetta, M., Cau, G., Puddu, P. and Serra, F., 2016. "A comparison between cfd simulation and experimental investigation of a packed-bed thermal energy storage system". *Applied Thermal Engineering*, Vol. 98, p. 1263âĂŞ1272. doi: 10.1016/j.applthermaleng.2016.01.019.

Çengel, Y.A., 2003. *Heat transfer: a practical approach*. McGraw-Hill.

Coutier, J. and Farber, E., 1982. "Two applications of a numerical approach of heat transfer process within rock beds". *Solar Energy*, Vol. 29, No. 6, pp. 451–462. doi:10.1016/0038-092x(82)90053-6.

Dominik Schilpf, Martin Stenglein, G.S., 2014. *Thermal storage CSP technology*. Projeto Energia Heliotérmica.

Hänchen, M., Brückner, S. and Steinfeld, A., 2011. "High-temperature thermal storage using a packed bed of rocks. heat transfer analysis and experimental validation". *Applied Thermal Engineering*, Vol. 31, No. 10, pp. 1798–1806. doi:10.1016/j.applthermaleng.2010.10.034.

Holman, J.P., 2010. *Heat transfer/ J. P. Holman*. McGraw Hill.

Incropera, F.P., 2013. *Fundamentals of heat and mass transfer*. Wiley.

Kuravi, S., Trahan, J., Goswami, D.Y., Rahman, M.M. and Stefanakos, E.K., 2013. "Thermal energy storage technologies and systems for concentrating solar power plants". *Progress in Energy and Combustion Science*, Vol. 39, No. 4, pp. 285–319. doi:10.1016/j.pecs.2013.02.001.

Mahmud, S., Islam, A.S. and Feroz, C., 2003. "Flow and heat transfer characteristics inside a wavy tube". *Heat and Mass Transfer*, Vol. 39, No. 5, p. 387âĂŞ393. doi:10.1007/s00231-002-0369-9.

Nield, D.A. and Bejan, A., 2006. *Convection in porous media*. Springer Science Business Media, Inc.

Nishimura, T., Bian, Y., Matsumoto, Y. and Kunitsugu, K., 2003. "Fluid flow and mass transfer characteristics in a sinusoidal wavy-walled tube at moderate reynolds numbers for steady flow". *Heat and Mass Transfer*, Vol. 39, No. 3, pp. 239–248. doi:10.1007/s00231-002-0304-0.

Rush, T., Newell, T. and Jacobi, A., 1999. "An experimental study of flow and heat transfer in sinusoidal wavy passages". *International Journal of Heat and Mass Transfer*, Vol. 42, No. 9, pp. 1541–1553. doi:10.1016/s0017-9310(98)00264-6.

Russ, G. and Beer, H., 1997. "Heat transfer and flow field in a pipe with sinusoidal wavy surface 1. numerical investigation". *International Journal of Heat and Mass Transfer*, Vol. 40, No. 5, pp. 1061–1070. doi:10.1016/0017-9310(96)00158-5.

Wang, C.C. and Chen, C.K., 2002. "Forced convection in a wavy-wall channel". *International Journal of Heat and Mass Transfer*, Vol. 45, No. 12, pp. 2587–259. doi:10.1016/s0017-9310(01)00335-0.

Zanganeh, G., Pedretti, A., Haselbacher, A. and Steinfeld, A., 2015. "Design of packed bed thermal energy storage systems for high-temperature industrial process heat". *Applied Energy*, Vol. 137, pp. 812–822. doi: 10.1016/j.apenergy.2014.07.110.

7. RESPONSIBILITY NOTICE

The authors are the only responsible for the printed material included in this paper.